# Supplemental Data

# The Retromer Coat Complex Coordinates Endosomal Sorting and Dynein-Mediated Transport, with Carrier Recognition by the *trans*-Golgi Network

**Thomas Wassmer, Naomi Attar, Martin Harterink, Jan R.T. van Weering, Colin J. Traer, Jacqueline Oakley, Bruno Goud, David J. Stephens, Paul Verkade, Hendrik C. Korswagen, and Peter J. Cullen**

## Table S1. All Clones Isolated as "Positive" Interactions from the Retromer SNX-BAR Yeast Two-Hybrid Analysis

| *Yeast two-hybrid bait* | *Identified interactor* | *Number of hits in screen* | *Accession number* |
|---|---|---|---|
| **Sorting nexin-1** | Sorting nexin-6 | 6 | AF121856 |
| | ADP-ribosylation factor-like 6 interacting protein 1 | 6 | NM_015161 |
| | Sorting nexin-5 | 5 | NM_152227 |
| | Yip1 domain family, member 5, YPT-interacting protein 1 A | 2 | NM_030799 |
| | RAB6 interacting protein 1 | 1 | NM_015213 |
| | neuronal pentraxin receptor | 1 | NM_014293 |
| | LOC152217 protein | 1 | XR_017713 |
| | zinc finger, ZZ-type containing 3, isoform CRA_e | 1 | NM_015534 |
| | suppressor of hairy wing homolog 2 | 1 | NM_080764 |
| **Sorting nexin-2** | Sorting nexin-6 | 3 | AF121856 |
| | Zinc finger CDGSH | 2 | NP_060934.1 |
| | Archain | 2 | NM_001655 |
| | Sorting nexin-5 | 1 | NM_152227 |
| **Sorting nexin-5** | Sorting nexin-1 | 24 | NM_003099 |
| | Sorting nexin-2 | 6 | NM_003100 |
| | CREB/ATF bZIP transcription factor | 5 | BC060807 |
| | p150glued | 4 | NM_004082 |
| | Sorting nexin-6 | 4 | AF121856 |
| | Sorting nexin-5 | 1 | NM_152227 |
| | Stathmin-2 (SCG10 protein) | 1 | AAV38837 |
| | CSE1 chromosome segregation 1-like protein | 1 | NM_001316 |
| **Sorting nexin-6** | p150glued | 16 | NM_004082 |

| | | | |
|---|---|---|---|
| | Sorting nexin-1 | 14 | NM_003099 |
| | Sorting nexin-2 | 6 | NM_003100 |
| | MLLT10 | 2 | NM_004641 |
| | Nudel | 2 | NM_001025579 |
| | creatine kinase, brain, isoform CRA_b | 1 | NM_001823 |
| | chromodomain helicase DNA binding protein 9, isoform CRA_b | 1 | CH471092 |
| | microtubule-associated protein 1B isoform 2 | 1 | NM_032010 |
| | zinc finger, A20 domain containing 2, isoform CRA_c | 1 | EAW62535 |
| | vacuolar H+ ATPase G1 | 1 | NM_004888 |
| | bromodomain adjacent to zinc finger domain, 2B, isoform CRA_c, homo sapiens | 1 | NM_013450 |
| | nephrocystin 3 | 1 | NM_153240 |
| | protein tyrosine phosphatase, receptor type, J, isoform CRA_d | 1 | NM_002843 |
| | CREB/ATF bZIP transcription factor | 1 | BC060807 |
| | PREDICTED: similar to angiomotin | 1 | XM_941912 |
| | C10orf78 protein [Homo sapiens] | 1 | NM_001002759 |
| | ADP-ribosylation-like factor 6 interacting protein 5 variant | 1 | NM_006407 |

**Table S2. Sirna Sequences Used during This Study**

| siRNA name | Target sequence |
|---|---|
| control | gacaagaaccagaacgcca |
| p150glued-I | ctggagcgctgtatcgtaa |
| p150glued-II | gaagatcgagagacagtta |
| p150glued-III | gctcatgcctcgtctcatt |
| Rab6IP1-I | gcacaaacctattatgaga |
| Rab6IP1-II | gcaaatcgtttcactcaga |
| Rab6IP1-III | gaacacctgcgtttagata |
| SNX1 | gaacaagaccaagagccac |

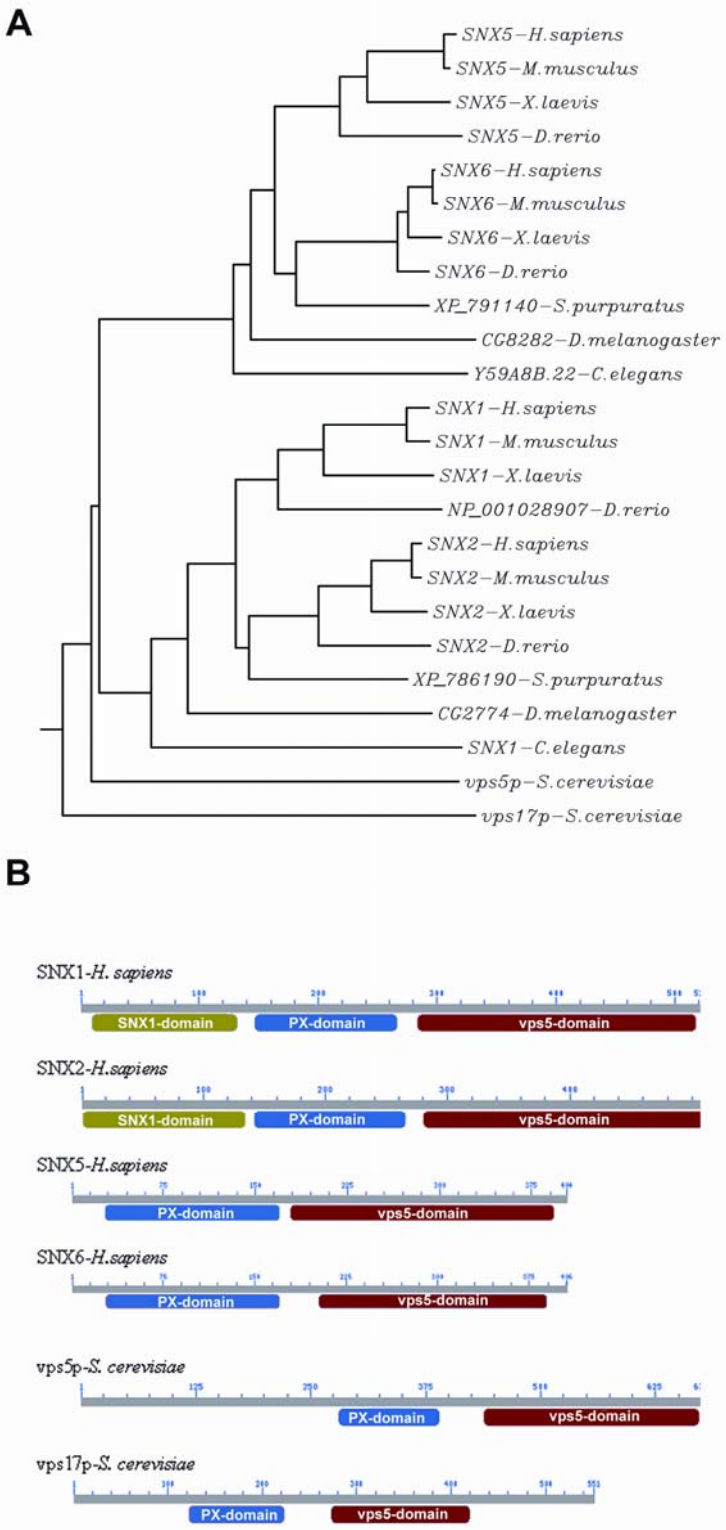


**Figure S1. Phylogenetic Analysis of Retromer Snxs Suggests that Vertebrate SNX1/SNX2 and SNX5/SNX6 Arose by Duplication from an Invertebrate SNX Gene Pair**

(A) Protein sequences of retromer SNXs of *Homo sapiens, Mus musculus, Xenopus laevis, Danio rerio, Strongylocentrotus purpuratus, Drosophila melanogaster, Caenorhabditis elegans* and *Saccharomyces cerevisiae* were either retrieved from databases or identified by blast searches. A Clustal W alignment was performed and a N-J tree constructed (http://align.genome.jp).

(B) Comparison of domain structure in the human and *S. cerevisiae* retromer SNXs.

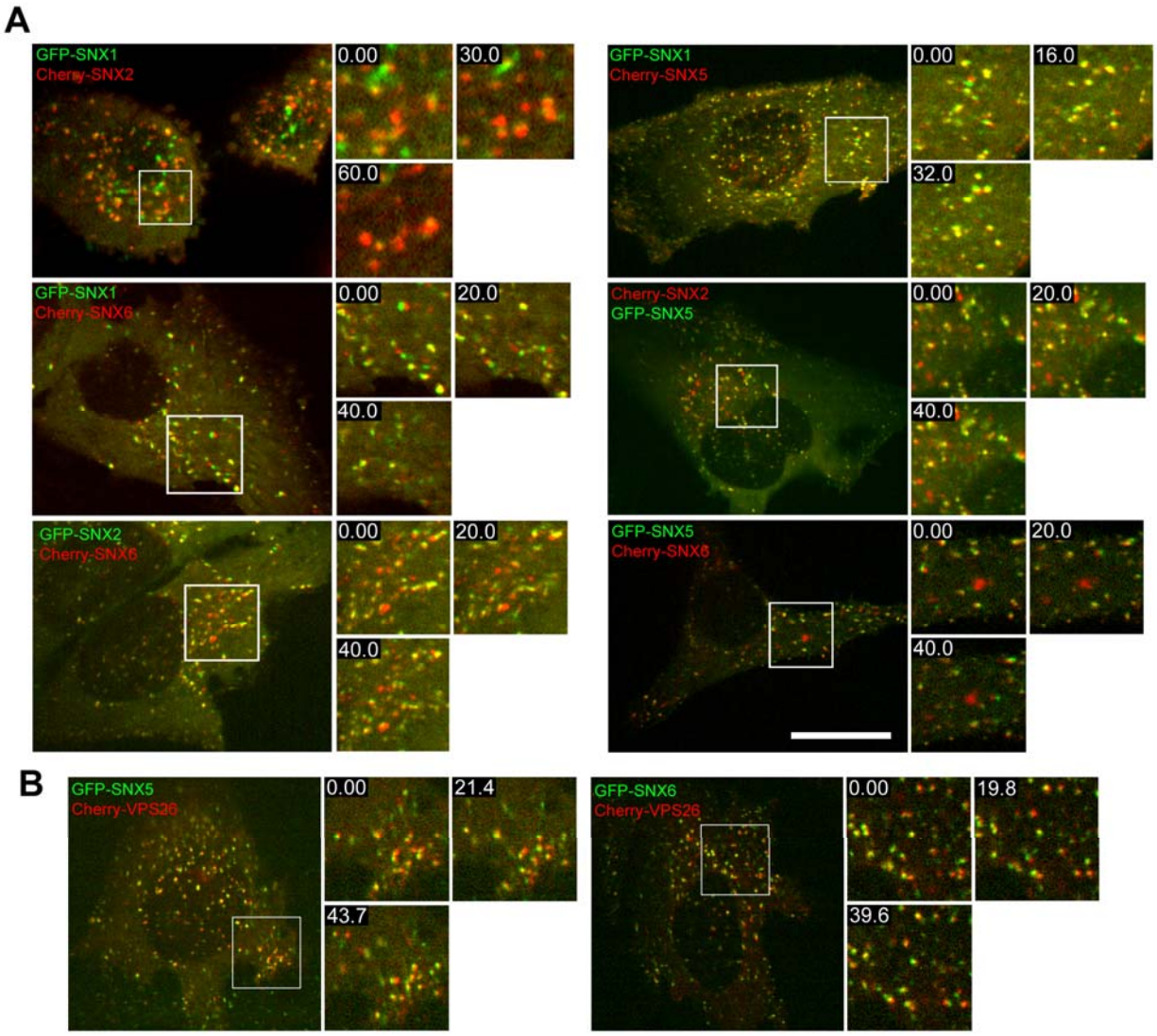


**Figure S2. Co-Expression of GFP or mcherry-Tagged Retromer Subunits Reveals High Degrees of Co-Localisation and Co-Movement**

(A) Co-localisation analysis was performed by co-expression of all possible pairings of the four retromer SNXs (SNX1, SNX2, SNX5 and SNX6) by lentiviral transduction of HeLa cells and live-cell imaging. In all SNX-combinations co-localisation and co-movement of vesicular structures can be detected. However, co-localisation is particularly pronounced for the combinations GFP-SNX1/mCherry-SNX5, GFP-SNX1/mCherry-SNX6, mCherry-SNX2/GFP-SNX5 and GFP-SNX2/mCherry-SNX6.

(B) Co-expression of a marker of the cargo-selective sub-complex of the retromer (mCherry-VPS26) with GFP-tagged SNX5 or SNX6 displays a high degree of co-localisation. Please note that the images in the GFP- and the mCherry-channel were collected sequentially, leading to the mCherry-channel being recorded with a short delay relative to the GFP-channel. Therefore the red and the green label on very fast moving structures appear to be separate, while most likely they reside on the same structure. Bar, 20 µm.

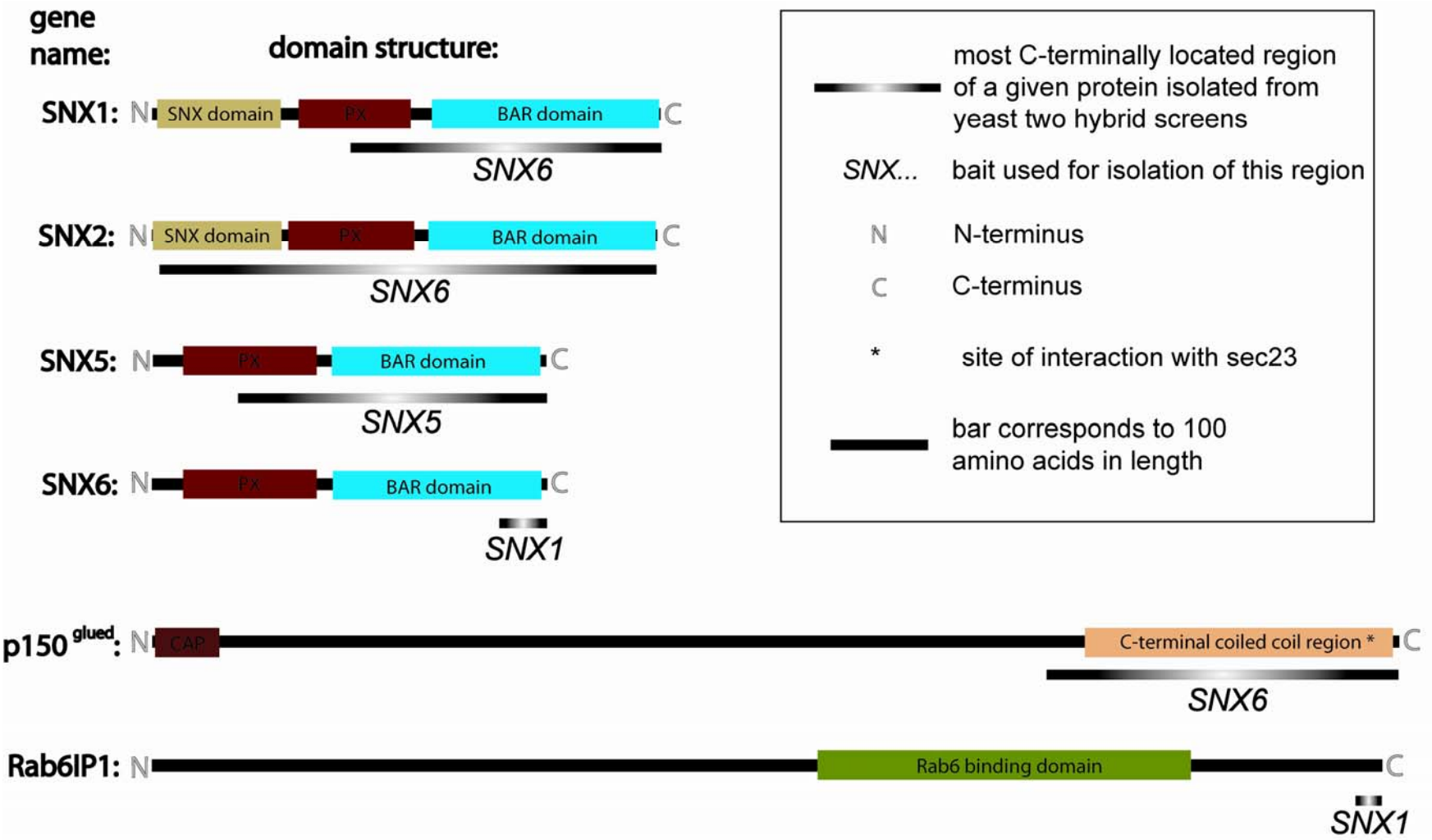


**Figure S3. Schematic Representation of Yeast Two Hybrid Hits with Identified Interaction Regions**

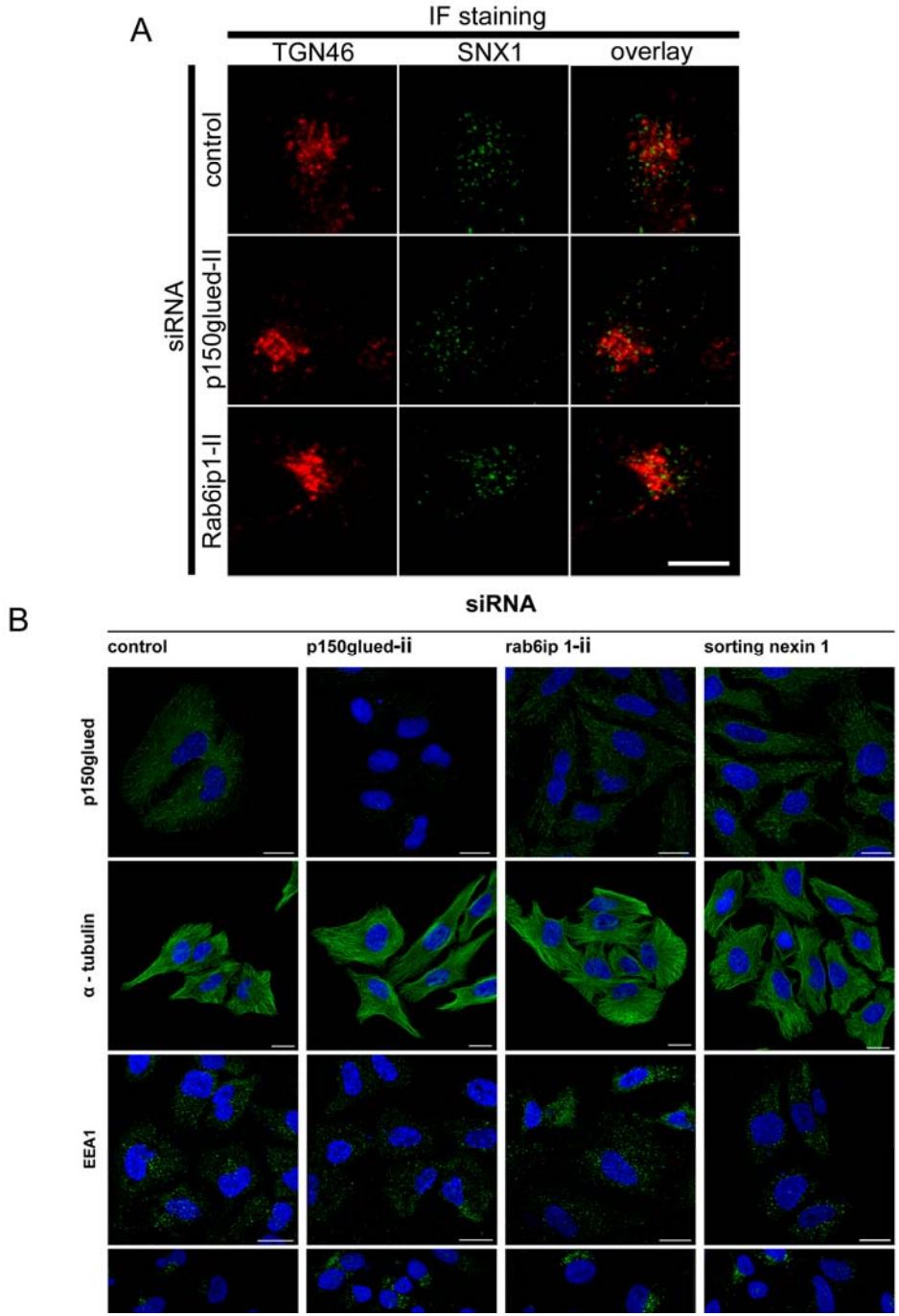
A
IF staining
TGN46
SNX1
overlay
siRNA
control
p150glued-II
Rab6ip1-II
B
siRNA
control
p150glued-ii
rab6ip 1-ii
sorting nexin 1
p150glued
α - tubulin
EEA1

**Figure S4. Cellular Organization upon p150$^{glued}$ and Rab6IP1 Suppression**
Under the level of p150$^{glued}$ or Rab6IP1 suppression achieved in the current study, the organisation of the TGN, as shown by labelling TGN46 is not grossly perturbed nor is the microtubule organisation or distribution of EEA1-positive early endosomes. A minor dispersal of the CD63-labelled lysosomal compartment is apparent upon p150$^{glued}$ suppression. Bars, 20 µm.

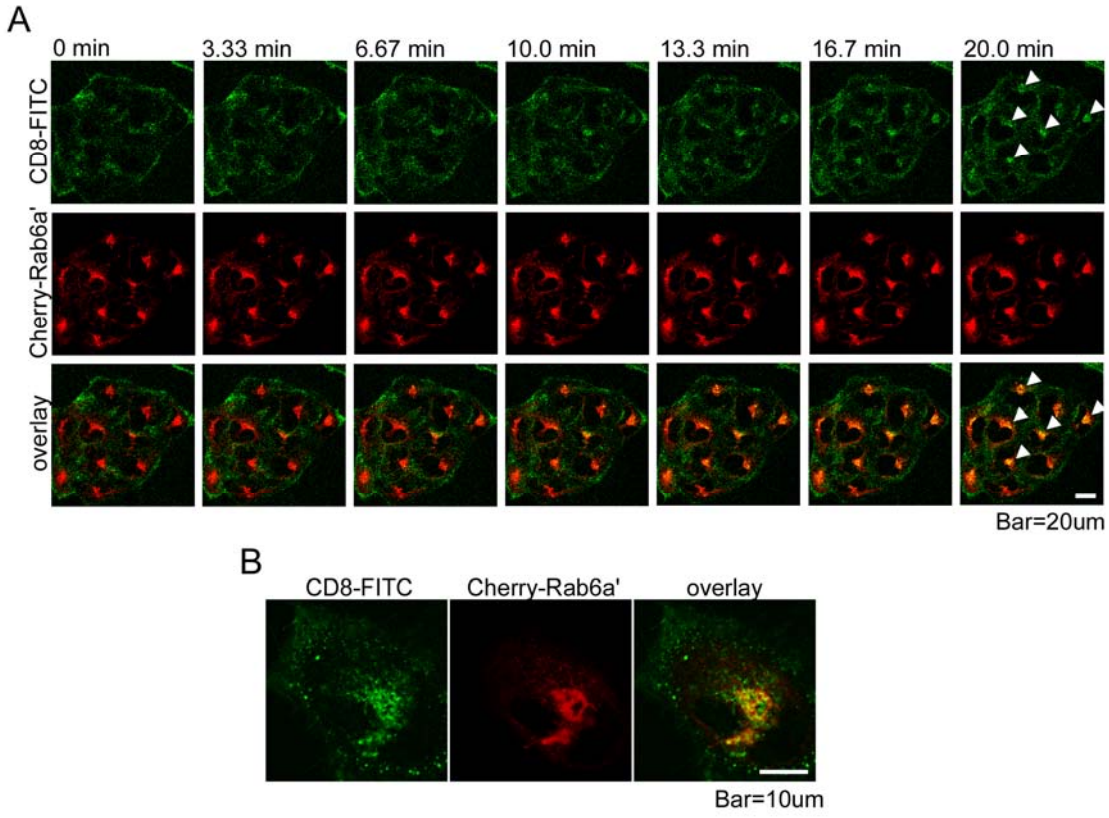


**Figure S5. Analyzing the Kinetics of CD8-CI-MPR Transport**
(A) CD8-tagged CI-MPR labelled with a CD8-FITC antibody travels from the plasma membrane via early endosomes to the TGN, as illustrated with stills taken from a 20 min movie. mCherry-Rab6a' labels the Golgi complex, arrowheads indicate CD8-FITC label concentration in the Golgi area (see Movie S2). Bar, 20 µm.
(B) Enlarged display of a HeLa cell after 20 min of CD8-FTIC uptake. Bar, 10µm.

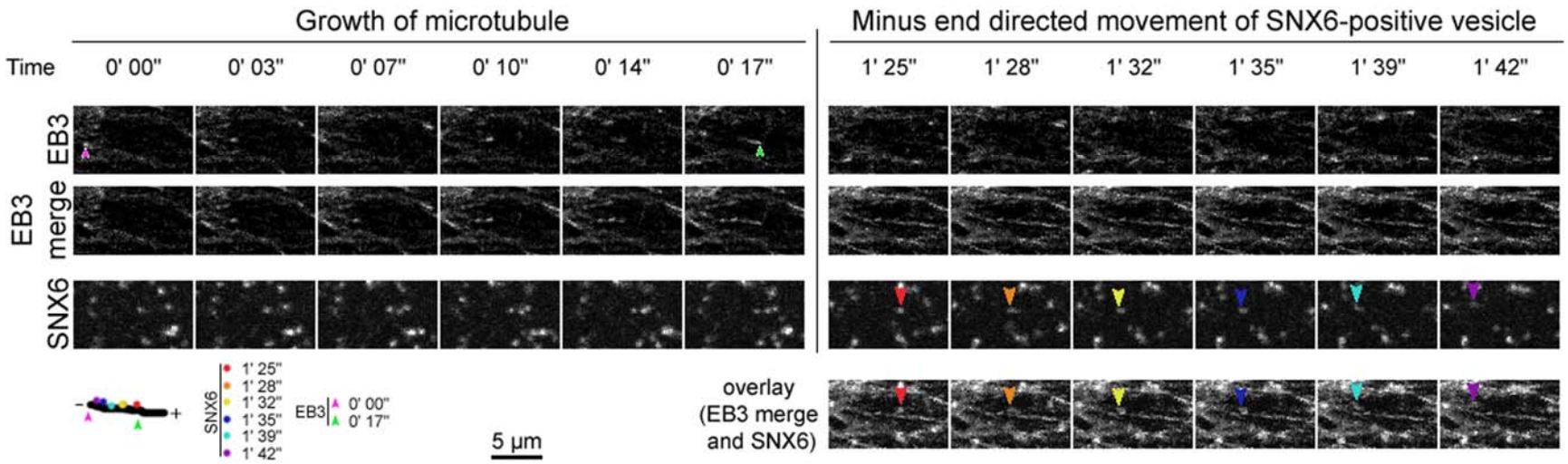


**Figure S6. SNX6-Labelled Endosomes Are Observed to Undergo Microtubule Minus-End Directed Movement**
Images captured from a movie examining the relationship between GFP-tagged EB3 (plus-end microtubule tracking protein) and mCherry-tagged SNX6. The selected region highlights the dynamic plus-end directed movement of GFP-EB3 for the time period shown as the microtubule grows from the point depicted by the pink arrow to that shown with the green arrow. Each individual frame is then merged (EB3 merge) to show the track and orientation of the microtubule (minus-end at the pink arrow, plus-end at the green arrow). During this period of growth SNX6-labelled endosomes are relatively static. At 1 minute and 25 seconds however, movement of a SNX6-labelled endosome (red arrow) is observed, which tracks stoichastically, at an average speed of approximately 0.35 µm/sec, towards the minus-end of the microtubule (shown by the various time-coded, coloured arrows). The overlay shows the combined images of the individual EB3 merge and SNX6 stills.

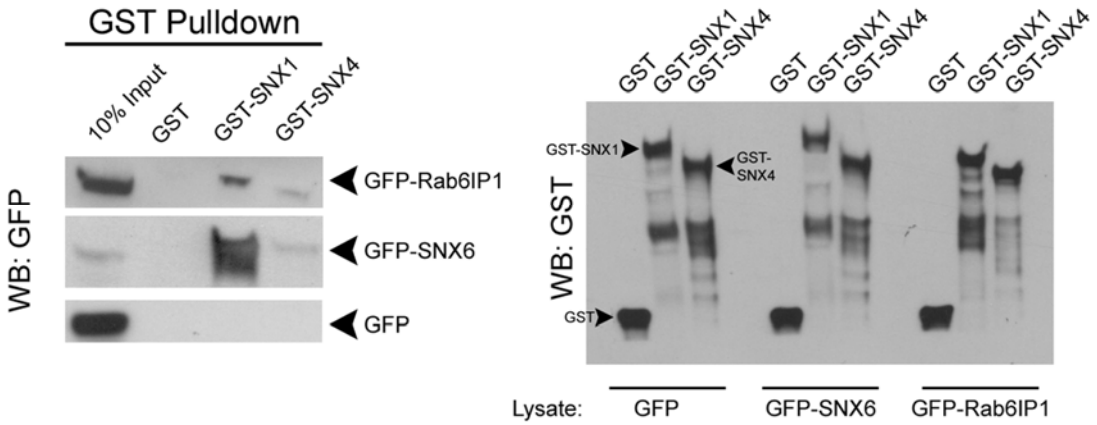


**Figure S7. Rab6IP1 Association Is Specific for SNX1 when Compared with SNX4**
GST pulldown of bacterially expressed SNX1 and SNX4 demonstrates that GST-SNX1 but not GST-SNX4 can associate with GFP-tagged Rab6IP1.

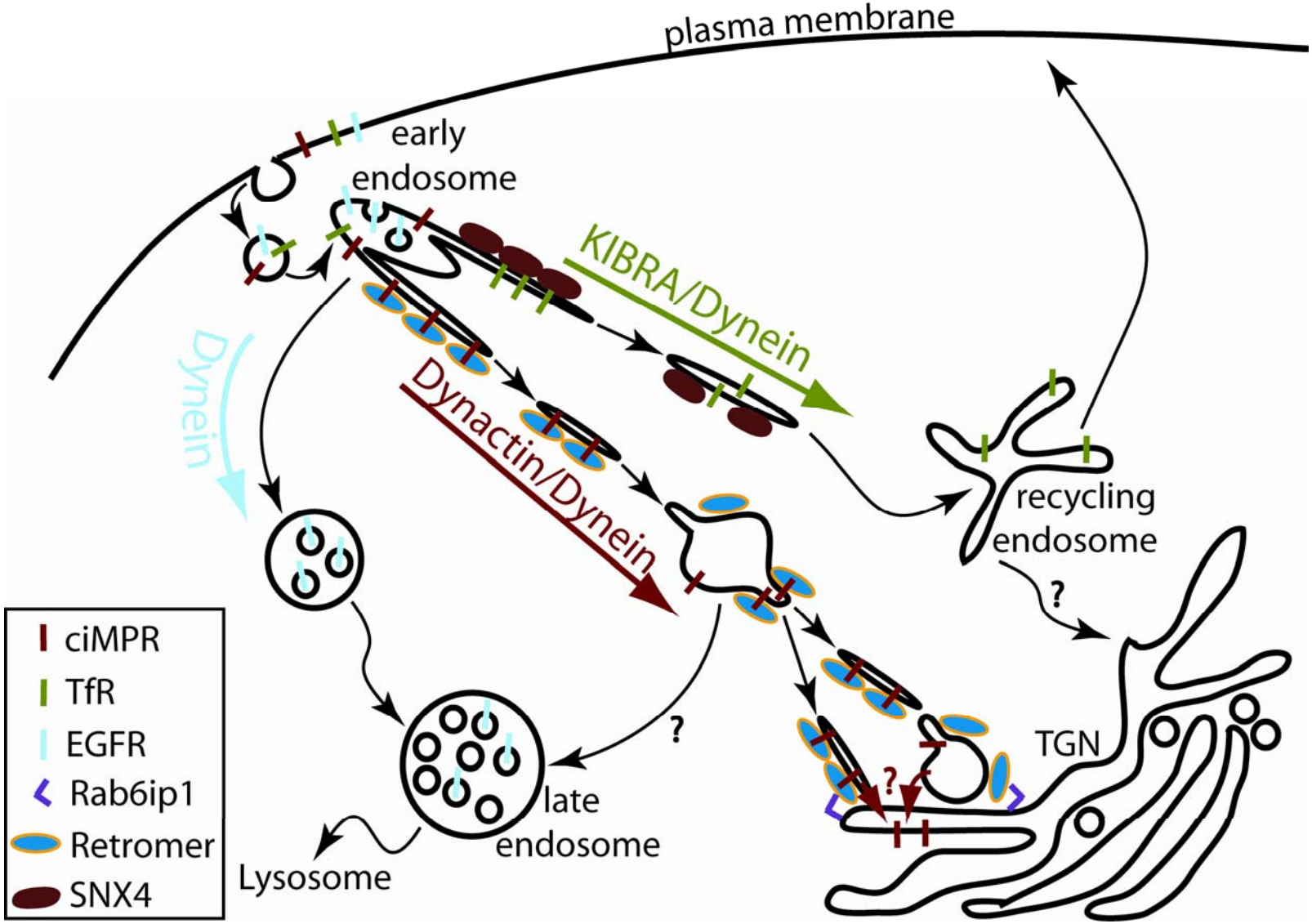


**Figure S8. Schematic Representation of s Model for Retromer-Mediated Endosomal Sorting**
In this model the involvement of the dynein-dynactin motor in retromer-mediated endosome-to-TGN transport is incorporated, as well as the putative tether Rab6IP1 located at the TGN. Also illustrated are the fusion and fission events of retromer-labelled endosomes visible in live cell imaging. Currently it is not clear what structures actually fuse with the TGN to deliver the CI-MPR (red

arrows indicated with ”?“). Integrated into this model are sorting of the transferrin receptor in a SNX4/KIBRA/dynein dependent pathway[25] and ESCRT mediated sorting of the EGF receptor towards the dynein dependent late endosome/lysosome pathway[44].